







## PAPER



Cite this: *Phys. Chem. Chem. Phys.*,  
2019, 21, 15576

# Tuning molecular dynamics by hydration and confinement: antiplasticizing effect of water in hydrated prilocaine nanoclusters†

G. N. Ruiz, <sup>ab</sup> I. Combarro-Palacios,<sup>b</sup> S. E. McLain, <sup>cd</sup> G. A. Schwartz, <sup>b</sup>  
L. C. Pardo, <sup>a</sup> S. Cerveny <sup>b</sup> and R. Macovez <sup>\*,a</sup>

In glass-forming substances, the addition of water tends to produce the effect of lowering the glass transition temperature,  $T_g$ . In a previous work by some of us (Ruiz *et al.*, *Sci. Rep.*, 2017, **7**, 7470) we reported on a rare anti-plasticizing effect of water on the molecular dynamics of a simple molecular system, the pharmaceutically active prilocaine molecule, for which the addition of water leads to an increase of  $T_g$ . In the present work, we study pure and hydrated prilocaine confined in 0.5 nm and 1 nm pore size molecular sieves, and carry out a comparison with the bulk compounds in order to gain a better understanding of the microscopic mechanisms that result in this rare effect. We find that the  $T_g$  of the drug under nanometric confinement can be lower than the bulk value by as much as 17 K. Through the concurrent use of differential scanning calorimetry and broadband dielectric spectroscopy we are able to observe the antiplasticizing effect of water in prilocaine also under nanometric confinement, finding an increase of  $T_g$  of up to almost 6 K upon hydration. The extension of our analysis to nanoconfined systems provides a plausible explanation for the very uncommon antiplasticizing effect, based on the formation of water-prilocaine molecular complexes. Moreover, this study deepens the understanding of the behavior of drugs under confinement, which is of relevance not only from a fundamental point of view, but also for practical applications such as drug delivery.

Received 29th March 2019,  
Accepted 21st June 2019

DOI: 10.1039/c9cp01771b

rsc.li/pccp

## 1 Introduction

Within the pharmaceutical industry finding the optimal form of a drug to administer to a patient is of paramount importance. Although crystalline phases present much higher kinetic stability than glassy materials, they also show a poor water dissolution profile.<sup>1</sup> The latter characteristic presents a major disadvantage since administration of drugs is very frequently mediated by dilution in water.<sup>2</sup> Avoiding phase transformation or change in physico-chemical properties during storage of a drug or of a formulation is vital, as is providing a drug formulated in a phase that can be easily absorbed by the body and is compatible with an aqueous medium. Studying the dynamics of glassy drugs and their interaction with water provides relevant

information not only for fundamental research, but may also lead to important pharmaceutical applications.

Water has been generally regarded as a universal plasticizer of foods and pharmaceutical products, in the sense that it serves to soften, or make less brittle, a hydrophilic or hygroscopic substance.<sup>3–6</sup> Hydration of glass-forming organic materials almost always leads to an increase of molecular mobility, which results in a lower glass-transition temperature  $T_g$  (the higher the water content, the lower the  $T_g$ ).<sup>7–10</sup> The reason for this is that the  $T_g$  of water<sup>11</sup> is lower than that of many other hydrophilic glass formers, and the  $T_g$  of a mixture tends to be intermediate to that of its components.<sup>12</sup> There are, to the best of our knowledge, only four reported cases of increase in  $T_g$  upon hydration, two of which were observed in large molecules, with one observation being the source of some controversy.<sup>13–15</sup> The first observation of a genuine antiplasticizing effect of water on the molecular mobility of a simple glass former, *N*-ethyl acetamide, was reported in 2014.<sup>15</sup>

Previous work by some of us has shown the occurrence of an antiplasticizing effect of water on the dynamics of a simple hydrogen-bonded molecular system, the pharmaceutically active molecule prilocaine.<sup>16</sup> Prilocaine (*N*-(2-methylphenyl)-2-(propyl-amino)propanamide, chemical formula  $C_{13}H_{20}N_2O$ ) is an amino-amide local anesthetic often used in dentistry, which shows

<sup>a</sup> Grup de Caracterització de Materials, Departament de Física, Universitat Politècnica de Catalunya, EEBE, Campus Diagonal-Besòs, Avenida Eduard Maristany 10-14, E-08019 Barcelona, Spain. E-mail: roberto.macovez@upc.edu

<sup>b</sup> Centro de Física de Materiales, (CSIC-UPV/EHU)-Material Physics Centre (MPC), Paseo Manuel de Lardizabal 5 (20018), San Sebastián, Spain

<sup>c</sup> Department of Biochemistry, University of Oxford, South Parks Road, Oxford OX1 3QU, UK

<sup>d</sup> Department of Chemistry, University of Sussex, Falmer, Brighton BN1 9RH, UK

† Electronic supplementary information (ESI) available. See DOI: 10.1039/c9cp01771b

maximum hydration at a mole fraction of  $x_{\text{H}_2\text{O}} = 0.33$ .<sup>17–19</sup> The addition of more water to the system separates the solution into two stable liquid phases: a prilocaine-rich liquid with minority water content (liquid  $L_1$ ,  $x = 0.33 \pm 0.02$ , with approximately two molecules of prilocaine for every  $\text{H}_2\text{O}$ ), and a very dilute water-based solution of prilocaine (liquid  $L_2$ ,  $x = 0.98 \pm 0.01$ , with approximately one molecule of prilocaine for every 99 molecules of  $\text{H}_2\text{O}$ ). The two phases are thermodynamically stable at ambient conditions.<sup>20</sup>

The antiplasticizing effect of water in prilocaine leads to a significant increase of  $T_g$  and of the structural relaxation time at fixed temperature, both of which increase with increasing water content, reaching a maximum at the saturation concentration corresponding to the  $L_1$  phase, which we will refer to as “hydrated prilocaine” in the following.<sup>16</sup>

The characterization of solutions under nanometric confinement, *e.g.* within the pores of molecular sieves, allows studying interfacial effects as well as the impact of size on the dynamics of amorphous systems. For instance, many drug delivery systems are based on the confinement of the pharmaceutical substance. By confining PLC and hydrated PLC ( $L_1$ ) inside the voids of nanoporous silicates it is possible to gain insight into the relaxation dynamics when only a few molecules are mutually interacting and an extended H-bond network cannot be formed. We carry out Broadband dielectric spectroscopy (BDS) and differential scanning calorimetry (DSC) measurements on pure and hydrated prilocaine, confined in molecular sieves of 0.5 and 1 nm pore size. We find that confinement leads to substantial lowering of the glass transition temperature, and that the antiplasticizing effect of water on the prilocaine matrix is systematically observed also in the confined system as in the bulk.<sup>16</sup> The current results point to the formation of PLC–water molecular aggregates as the cause of the observed increase of  $T_g$  upon hydration.

## 2 Sample preparation and experimental techniques

### 2.1 Sample preparation

Prilocaine hydrochloride salt was purchased from Sigma Aldrich and reacted to form the free base prilocaine, as described previously.<sup>21,22</sup> The water-saturated prilocaine liquid  $L_1$  was obtained by mixing equal amounts of purified water and pure prilocaine, and keeping the mixture in the liquid state in a thermal bath at 323 K for 2 days. This allowed the system to separate into the two thermodynamically stable phases, namely a prilocaine-rich ( $L_1$ ) and a water-rich ( $L_2$ ) solution.

Molecular sieves also purchased from Sigma Aldrich were used as confining environment. Molecular sieves are made of metal aluminosilicates forming a 3D network of alumina and silica tetrahedra with irregular pores that do not have a defined geometry, but present an average effective diameter of either 0.5 or 1 nm. The molecular composition of the 0.5 nm molecular sieves is  $\text{CaNa}_{12-2n}[(\text{AlO}_2)_{12}(\text{SiO}_2)_{12}] \cdot x\text{H}_2\text{O}$ , while molecular sieves of 1 nm pore size are composed of sodium aluminum silicates.

In order to ensure that no water was initially present inside the confining material, the beads were dried in a vacuum oven at 353 K for two days. The dried molecular sieves were then immersed into different containers with pure and hydrated prilocaine, respectively. The whole process was carried out inside a sealed vacuum glove box, in order to prevent unwanted hydration of the molecular sieves. The flasks were hermetically sealed and kept at a temperature of 318 K for two months, in order to allow the liquid to penetrate into the nanometric pores of the molecular sieves.

With the aim of ensuring that the BDS and DSC measurements did not contain any contribution from the bulk solutions, the outer surfaces of the filled molecular sieves were cleaned by briefly immersing the beads in ethanol, and then quickly drying them with tissue paper.

Six distinct types of samples were studied with each technique: bulk prilocaine, bulk hydrated prilocaine, confined prilocaine (0.5 and 1 nm), and confined hydrated prilocaine (0.5 and 1 nm); for comparison purposes, we characterized also the empty molecular sieves.

### 2.2 Experimental techniques

**2.2.1 Differential scanning calorimetry.** A differential scanning calorimeter DSC TA Instrument Q2000 was used in standard mode to measure the glass transition and exclude the occurrence of crystallization of the water in the nanoconfined samples. Hermetic aluminum pans were employed, with sample weights of about 10 mg. In the case of confined samples, empty and dried molecular sieves were used as reference. A heating/cooling rate of  $8 \text{ K min}^{-1}$  was employed. All samples were melted inside the DSC by keeping them at 313.5 K for 5 minutes and subsequently cooled to 203.15 K followed by an annealing to enhance the visibility of the calorimetric signal of the glass transition, as done in our previous work.<sup>16</sup> The annealing temperature was set to 215.2 K for bulk and 0.5 nm samples (as done in ref. 16), and 203.5 K for 1 nm samples, chosen so as to perform the annealing about 5 K below  $T_g$ . The details of the latter protocol can be found in the supplementary material.

**2.2.2 Broadband dielectric spectroscopy.** Broadband dielectric spectroscopy measurements were carried out in the frequency range  $10^{-2}$ – $10^6 \text{ Hz}$  with a Novocontrol Alpha analyzer. The samples were placed between parallel gold-plated electrodes with a diameter of 30 mm. The sample temperature was controlled inside a cryostat with stability better than 0.1 K. The capacitors were initially heated to 323 K to ensure that the drug was in the liquid state. The cryostat of the impedance analyzer was precooled to 200 K prior to the insertion of the sample holder where the capacitor is mounted. Isothermal frequency scans recording the complex dielectric permittivity were performed by increasing the sample temperature from 200 K in a stepwise fashion, with steps of 2 or 3 K (depending on the temperature range) until ambient temperature was reached. Measurements on empty molecular sieves were performed every 5 K from 140 K to 300 K.

**2.2.3 FTIR ATR.** To gain further insight into the composition of the intercalated liquids, attenuated-total-reflectance Fourier-transform infrared (ATR-FTIR) measurements were performed at

room temperature in the range of 4500–1000  $\text{cm}^{-1}$ . Each spectrum was collected with a resolution of 4  $\text{cm}^{-1}$  and an average of 150 repetitive scans. The spectra were baseline corrected by using the Software Spectra Analysis from Jasco, and no smoothing of the data was done. The molecular sieves were crushed and pulverized in a mortar and the bulk liquids were used as prepared.

## 3 Results

### 3.1 DSC results

The DSC scans measured upon heating at 8  $\text{K min}^{-1}$  on both bulk and confined prilocaine (hereafter, PLC) are shown in Fig. 1. Panel (a) shows bulk samples and panels (b) and (c) show samples confined in 1 nm and 0.5 nm pore size molecular sieves (MS), respectively. The red traces correspond to pure PLC, the blue traces are the hydrated PLC samples (as mentioned previously, hereafter the term hydrated PLC stands for the equilibrium liquid  $L_1$ , which corresponds to the solubility limit of water in prilocaine). Gray dotted lines are the tangents used to obtain the onset glass transition temperatures,  $T_g$ , which are found to be  $221.4 \pm 0.5$  K and  $225.3 \pm 0.5$  K for the pure and hydrated bulk samples, respectively, consistent with our previous results.<sup>16</sup> This confirms the antiplasticizing effect of water on bulk prilocaine, since an increase of about 4 K is produced upon hydration.

First, we analyze the effect of water on the glass transition of PLC in bulk and confined systems. In all cases we observe an increase of  $T_g$  upon hydration. This effect amounts to 3.9 K in the bulk material, 2.6 K for samples confined in 0.5 nm pores and is even larger (5.6 K) for samples confined in 1 nm pores. Thus, the antiplasticizing effect exerted by water in the bulk is also observable under confinement. From this observation we can conclude that the interfacial interactions on the samples under confinement are not strong enough to break the antiplasticizing effect of water.

Next, we analyze the effect of nanometric confinement on the glass transition of neat PCL. The  $T_g$  of confined PCL is lower

than that of the bulk material (the values are 221.4 K for bulk and 216.3 and 204.9 K for confined samples in 0.5 and 1 nm, respectively). The observation in the filled MS of a glass transition temperature similar to that of bulk prilocaine proves that prilocaine-containing clusters are present within the pores; this is also confirmed by our BDS (Section 3.2) and FTIR-ATR (Section 3.4) results. The lower  $T_g$  values under confinement with respect to the bulk confirm that the confined clusters do not have a large number of interactions with the walls of the MS (a strong interaction with the walls would cause an increase of the glass transition temperature). This is also consistent with the behavior discussed above. Therefore, we can conclude that in these systems the surface interaction effects are less important than the size confinement effects.

### 3.2 BDS results

Pure and hydrated PLC confined in MS of 0.5 and 1 nm pore size were characterized by BDS. Pristine and hydrated bulk PLC were also characterized under the same experimental conditions, for comparison purposes.

Fig. 2 shows the dielectric loss spectra of PLC confined in 0.5 nm MS for temperatures ranging from 243 to 258 K. Just as in the bulk case displayed in Fig. 3(a), a prominent relaxation peak can be identified in the high frequency spectral region, which shifts to higher frequencies with increasing temperature. In addition to this peak, a shoulder is visible in the low-frequency portion of the spectrum; this second relaxation loss is an interfacial effect due to the intrinsic heterogeneity of the confined sample, as will be discussed in detail below.

The dielectric loss spectra of both bulk samples were fitted as the sum of an Havriliak–Negami relaxation process and a background proportional to reciprocal frequency representing the dc conductivity, as done previously.<sup>16</sup> The fit components are represented in panel (a) of Fig. 3 for bulk PLC at 240 K.

In the case of the dried (empty) molecular sieves of 0.5 nm pore size, two Cole–Cole functions and a conductivity background were needed to account for all spectral features. The two relaxations are likely to be interfacial dielectric relaxation

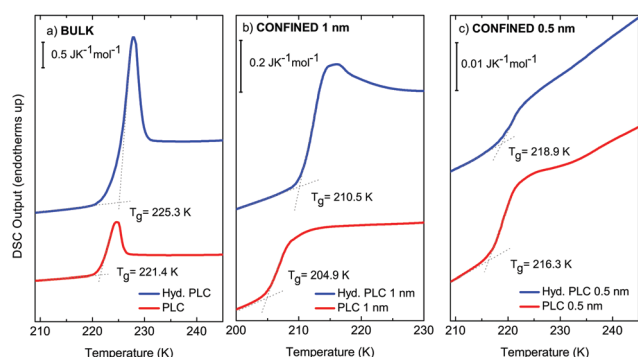


Fig. 1 DSC scans measured upon heating at 8  $\text{K min}^{-1}$ . (a) Bulk samples (b) 0.5 nm pore size confinement (c) 1 nm pore size confinement. In all cases red traces indicate pure PLC, whereas blue traces portray hydrated PLC samples. Gray dotted lines indicate the tangents used to identify the onset glass transition temperature,  $T_g$ . All  $T_g$  values have an error of  $\pm 0.5$  K.

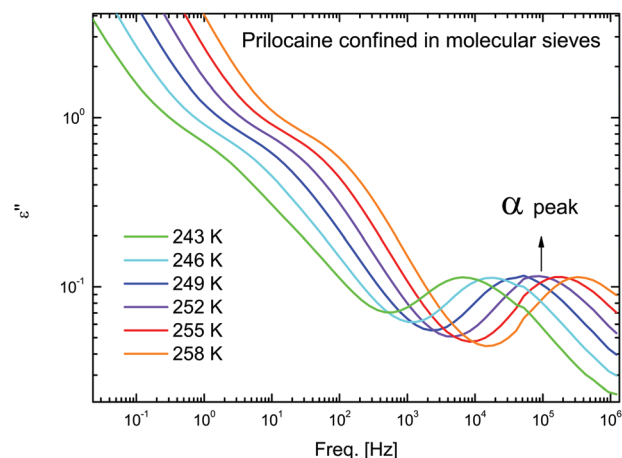
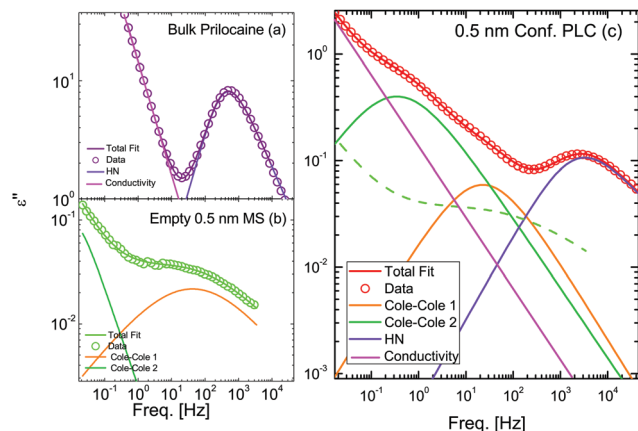


Fig. 2 Isothermal dielectric loss spectra ( $\epsilon''$ ) of pure prilocaine confined in molecular sieves of 0.5 nm pore size between 243 and 258 K, every 3 K.



**Fig. 3** Dielectric loss spectra at 240 K. Empty dots represent data points and the overlapping traces indicate the total fit, sum of the fit components used for each measurement. (a) Bulk PLC. An HN profile (violet) fits the primary  $\alpha$  relaxation and a conductivity background (pink) is added. (b) Empty molecular sieves (0.5 nm). Two Cole–Cole functions (orange and green) are needed to fit the spectrum. (c) Confined PLC (0.5 nm). Two Cole–Cole processes (orange and green full line), added to an HN relaxation (violet full line) and conductivity (pink full line). The green dashed line is the loss spectrum of the empty molecular sieves of panel (b), shown for direct comparison.

processes arising from the space-charge polarization caused by accumulation of charges at regions with different characteristics (conductivity, permittivity) such as the aluminosilicate, the empty pores and the macroscopic interstitial space between molecular sieves. Fig. 3b shows the fit components for the empty molecular sieves measured at 240 K and the corresponding total fit. Of the two spectral features observed in the empty MS, the most intense one is observed at lower frequency, and as shown below it corresponds to a conductivity relaxation at the inner surface of the empty pores. Concerning the higher frequency relaxation (visible as a peak in Fig. 3(b)), comparison with the data of Jansson *et al.*<sup>23</sup> on hydrated MS samples (see ESI†) indicates that this faster relaxation is probably an interfacial relaxation due to a minority fraction (less than 7%) of small pores which still contain water after our thermal treatment. In fact, we observed the same relaxation in the MS samples filled with pure or hydrated prilocaine (see below). This indicates that such pores are small enough to trap and retain water molecules, and are instead inaccessible to the prilocaine moiety. Interfacial water-related relaxations are well known to occur in partially hydrated organic and inorganic samples<sup>24,25</sup> and in hydrated MS.<sup>26</sup> Their origin is debated, but they may be space-charge relaxations involving protonic charge carriers.<sup>27</sup>

Three relaxation peaks were identified in the spectra of prilocaine under 0.5 nm confinement, as shown in Fig. 3(c) for  $T = 240$  K. The relaxation observed at highest frequency was fitted with a HN function, as the  $\alpha$  relaxation of bulk prilocaine.<sup>16</sup> The other two peaks were fitted with Cole–Cole functions and correspond to the interfacial processes already observed in the empty molecular sieves (panel (b)). The strength of the HN process depends on several factors that are difficult to quantify, such as the size and geometry of the pores, and the number of pores successfully filled

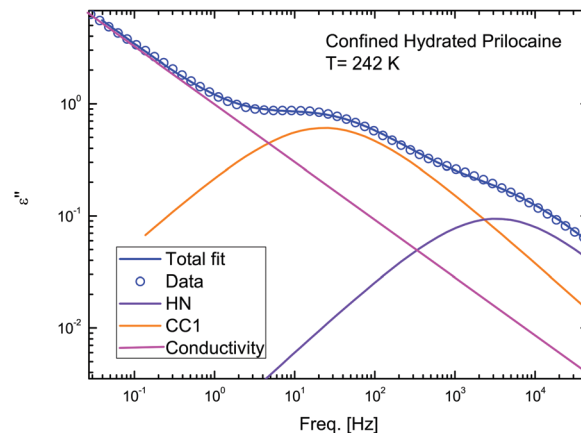


**Fig. 4** Data (empty circles) and fit (full lines) of the dielectric loss spectra of hydrated PLC confined in molecular sieves (0.5 nm) obtained at 242 K. The orange trace portrays the Cole–Cole function used to fit the data, while the violet and pink traces show the HN and conductivity contributions respectively.

with solution. The green dashed line of Fig. 3 shows the data of the empty molecular sieves of panel (b) for direct comparison. It can be observed that not only the dielectric signal is qualitatively different, but also the overall loss intensity of the empty sieves is considerably smaller than when they are filled with prilocaine.

The data of all other confined samples (hydrated PLC under 0.5 and 1 nm confinement, and pure PLC under 1 nm confinement) were fitted using a HN function, one Cole–Cole function and a dc conductivity contribution. Fig. 4 shows (empty circles) the experimental loss spectrum of PLC under 0.5 nm confinement at 242 K, together with the overall fit and individual fit components. The data and fitting curves of PLC confined in 1 nm pores are shown in the ESI†.

### 3.3 Analysis of the relaxation times

Fig. 5 shows the relaxation time  $\tau$  extracted from the fit procedure for bulk and 0.5 nm confinement as a function of the inverse temperature (Arrhenius plot). Full red and blue markers correspond to pure and hydrated PLC under confinement, respectively, whereas empty markers of the same colors portray the bulk substances. As visible in the figure, the fastest (highest-frequency) relaxation process exhibits characteristic times that are close to those of the primary structural relaxation of pure and hydrated bulk PLC. In view of this similarity, it is natural to assign the fastest relaxation in the confined material to the structural relaxation of PLC under confinement. This is corroborated by the comparison of calorimetric and dielectric glass transition temperatures (see below). Green markers are relaxation times of the empty molecular sieves. Violet stars represent the so-called conductivity relaxation time of the empty molecular sieves, defined as the inverse of the angular frequency at which the imaginary part of the dielectric modulus,  $M''$ , displays a maximum. The spectral position of this maximum coincides with the kink in the real part of conductivity,  $\sigma'$ , that signals the onset of the electrode polarization effect<sup>28</sup> (see ESI†), and with the relaxation time of the slower and more intense relaxation of the empty molecular sieves. This confirms that the slower



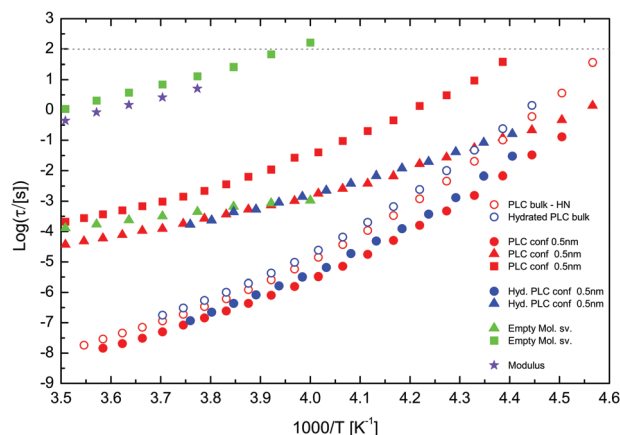


**Fig. 5** Arrhenius plot of the relaxation times  $\tau$  of the fitting functions for bulk and 0.5 nm MS. Full red and blue markers correspond to pure and hydrated PLC under confinement, respectively, whereas empty markers of the same colors portray the bulk substances. Green markers are relaxation times of the empty molecular sieves. Circles represent HN functions, squares and triangles CC functions. Violet stars represent the relaxation time associated to the maximum of the complex part of the dielectric modulus,  $M''$ , of the empty molecular sieves.

relaxation of the empty molecular sieves is an interfacial space-charge relaxation.

In Fig. 5 it may be observed that the relaxation times of the CC1 fit component of the confined samples (blue and red and triangles) are very similar to one another, and they moreover overlap with those of the faster relaxation time in the empty MS. This strongly suggests that the same relaxation is present in the MS after soaking them in prilocaïne; in other words, the CC1 fit component corresponds to the minority fraction of tiny pores which contain tightly bound, trapped water, which are retained also after prilocaïne has entered the larger pores. When the pores of the molecular sieves are filled by a substance, the conductivity relaxation time abruptly changes because of the conductivity and polarization contribution of the PLC or PLC–H<sub>2</sub>O inside the pores. The relaxation observed in the empty MS as the green squares in Fig. 5, which we have assigned to a space-charge relaxation at the inner surface of the MS, could be shifting to shorter times when the pores are filled, with prilocaïne, which would rationalize the observation of the CC2 relaxation (red squares) at different relaxation times compared with the empty MS (green squares). Regardless of the specific mechanisms giving rise to the relaxations observed as CC functions, it is clear that all CC relaxations observed correspond to interfacial effects and that they are not true molecular relaxation processes (as is instead the structural  $\alpha$  relaxation) of the confined material.

The structural  $\alpha$  relaxation times of all samples are compared in Fig. 6. Full red and blue dot markers correspond to pure and hydrated PLC in the 0.5 nm MS, respectively, whereas empty square markers of the same colors portray the bulk substances and empty triangles the 1 nm MS samples. The temperature dependence of the  $\alpha$  relaxation was fitted in all cases using the Vogel–Fulcher–Tammann (VFT) function given by<sup>29</sup>

$$\tau_{\alpha}(T) = \tau_{\infty} \exp[DT_{VF}/(T - T_{VF})] \quad (1)$$

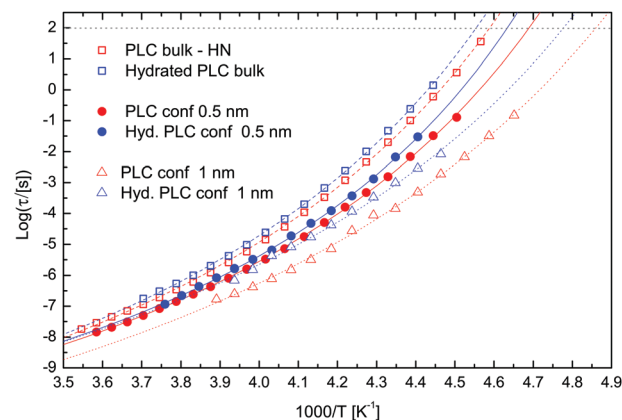


**Fig. 6** Arrhenius plot of the relaxation times  $\tau$  of the HN fitting functions for bulk, 0.5 nm MS and 1 nm MS samples. Full red and blue dot markers correspond to pure and hydrated PLC in the 0.5 nm MS, respectively, whereas empty square markers of the same colors portray the bulk substances and empty triangles the 1 nm MS samples. Continuous and dotted lines are VFT fits (eqn (1)).

where the prefactor  $\tau_{\infty}$ , the strength parameter  $D$  and the so-called Vogel–Fulcher temperature  $T_{VF}$  are phenomenological constants.

The extrapolated  $T_g$  values, estimated as the temperature at which the relaxation time equals 100 s (dashed horizontal line in Fig. 6), are  $217.9 \pm 0.5$  K for pure bulk prilocaïne, and  $219.7 \pm 0.5$  K for hydrated bulk prilocaïne. The value for pure PLC coincides with that reported by Wojnarowska *et al.*<sup>30</sup> The small difference (approximately 0.4 K) between the present results and those obtained in our previous work<sup>16</sup> is smaller than the experimental error. Table 1 displays the dielectric  $T_g$  values, together with the calorimetric glass transition temperatures for comparison.

The  $T_g$  values obtained by this method are compatible with those found from the DSC measurements, taking into account that in BDS the cooling of the liquid sample is done at a faster rate while heating takes place in discontinuous steps. The similarity between the dielectric vitrification temperatures and the calorimetric  $T_g$  values confirm our identification of the fastest relaxation of pure and hydrated PLC under confinement as the structural relaxation of these samples. This entails that water exerts a direct antiplasticizing effect on the molecular relaxation dynamics of to PLC not only in the bulk, but also in the small clusters that can fit inside pores of 0.5 and 1 nm diameter.

**Table 1** Onset  $T_g \pm 0.5$  K and extrapolated  $T_g \pm 0.5$  K at 100 s, obtained by DSC and BDS respectively, for bulk and confined samples of PLC and hydrated PLC

Sample	$T_g$ [K] (DSC)	$T_g$ [K] (BDS)
Bulk PLC	221.4	217.9
Bulk Hyd. PLC	225.3	219.7
Conf. 0.5 nm PLC	216.3	213.1
Conf. 0.5 nm Hyd. PLC	218.9	216.0
Conf. 1 nm PLC	204.9	205.8
Conf. 1 nm Hyd. PLC	210.5	209.7

**Table 2** VFT fit parameters of the structural relaxation of all studied samples, together with the kinetic fragility index,  $m$ 

Sample	$T_{VF}$ [K]	$\log(\tau_{\infty}/[s])$	$D \pm 1$	$m$
Bulk PLC	$174 \pm 2$	$-15 \pm 1$	10	$80 \pm 13$
Bulk Hyd. PLC	$173 \pm 1$	$-15 \pm 1$	10	$80 \pm 9$
0.5 nm PLC	$171 \pm 2$	$-14 \pm 1$	8	$84 \pm 16$
0.5 nm Hyd. PLC	$177 \pm 3$	$-14 \pm 1$	9	$83 \pm 13$
1 nm PLC	$159 \pm 6$	$-15 \pm 1$	10	$74 \pm 26$
1 nm Hyd. PLC	$164 \pm 4$	$-14 \pm 1$	12	$74 \pm 22$

Table 2 shows the VFT fit parameters of the structural relaxation (eqn (1)) of all studied samples, together with the kinetic fragility index  $m$ , which is defined as<sup>31</sup>

$$m = \frac{D}{\ln(10)} \frac{T_{VF}}{T_g} \left(1 - \frac{T_{VF}}{T_g}\right)^{-2} \quad (2)$$

The fragility index for the bulk samples of PLC and hydrated PLC is in agreement with previous studies.<sup>16,30</sup> It can be observed that the fragility index is virtually unchanged within experimental error regardless of hydration or confinement, despite the significant changes in glass transition temperature.

### 3.4 FTIR ATR

Fig. 7(a) displays the FTIR spectra of bulk and confined prilocaine and bulk and confined hydrated prilocaine. The spectra of the empty molecular sieves are also shown for comparison, whereby it is seen that the most intense absorption band of the confined samples, centered around  $950\text{ cm}^{-1}$ , is actually due to the molecular sieves themselves. For comparison purposes, we have normalized all FTIR spectra, except those of the bulk prilocaine liquids, to the intensity of this band.

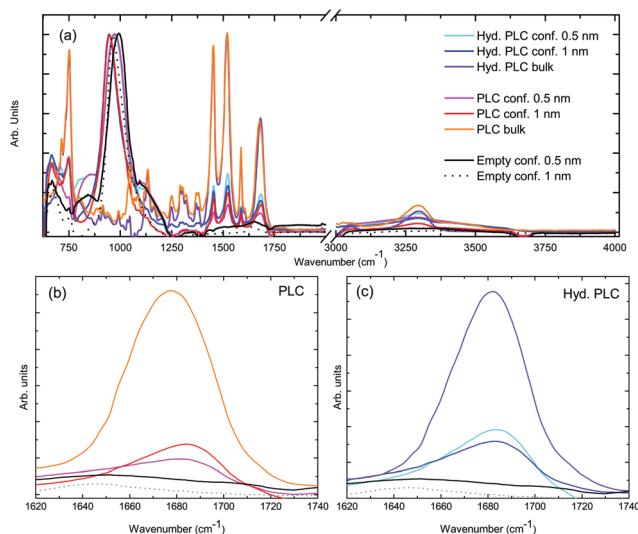


**Fig. 7** (a) FTIR spectra of bulk and confined PLC and hydrated PLC. PLC samples in 0.5 nm, 1 nm confinement and in bulk are indicated by the pink, red and orange traces respectively. Hyd. PLC samples in 0.5 nm, 1 nm confinement and in bulk are indicated by cyan, blue and violet traces respectively. Black trace indicates empty 0.5 nm and dotted line 1 nm. (b) C=O vibration of empty and PLC samples. (c) C=O vibration of empty and hyd. PLC samples.

The characteristic spectral features of bulk prilocaine, namely the band at  $750\text{ cm}^{-1}$  and the series of peaks in the range between  $1400$  and  $1700\text{ cm}^{-1}$ , are observed in all FTIR spectra, including bulk hydrated prilocaine and all confined samples. These results confirm the presence of prilocaine inside the pores.

The only significant spectral difference observed in the spectra concerns the position of the C=O stretching mode around  $1680\text{ cm}^{-1}$ , which is shown in detail in the lower panels of Fig. 7. We have shown in our previous work<sup>16</sup> that the oxygen atom in the carbonyl group is directly involved in the formation of intermolecular hydrogen bonds (e.g. of prilocaine with water).

As may be seen in Fig. 7(b), in the case of pure (anhydrous) prilocaine the C=O vibration shifts systematically under the effect of confinement, from  $1677\text{ cm}^{-1}$  in the bulk liquid to  $1681$  and  $1684\text{ cm}^{-1}$  under 1 nm and 0.5 nm confinement, respectively. This shift might signal the loss of intermolecular prilocaine–prilocaine bonds under confinement.

On the other hand, we observe almost no shift in the frequency of the C=O mode in the case of hydrated prilocaine (Fig. 7(c)), and its spectral position is at any rate independent of nanoconfinement size (the C=O mode shifts from  $1681\text{ cm}^{-1}$  in the bulk  $L_1$  liquid to  $1683\text{ cm}^{-1}$  under both 1 nm and 0.5 nm confinement). This suggests that the water–prilocaine interaction is not strongly modified under confinement.

## 4 Discussion

### 4.1 Bulk vs. confined dynamics

For PLC and hydrated PLC the  $T_g$  values under confinement inside the 0.5 nm pores of the molecular sieves are lower – between 4.9 and 6.4 K with respect to the bulk system. In the case of 1 nm MS the effect observed in  $T_g$  with respect to bulk samples is even larger: when confined in such pores  $T_g$  decreases as much as 12 K in the case of PLC and 10 K for hydrated PLC. This effect is consistently observed with both experimental techniques employed. Such a decrease in the glass transition temperature upon confinement implies there are no strong interactions between the drug and the walls of the molecular sieves, as this would instead quench the dynamics and lead to higher  $T_g$  values. The observed changes in the  $\alpha$  relaxation therefore arise mainly from the dynamics of PLC–PLC and PLC–H<sub>2</sub>O aggregates, and not from their interaction with the inner pore surface.

The reason for this lowering in  $T_g$  is likely the reduction of the size of cooperatively rearranging clusters upon confinement. In the bulk system, prilocaine and water molecules are linked through hydrogen bonds.<sup>22</sup> Under confinement, the characteristic size of the H-bonded clusters (e.g. prilocaine molecules bridged by water) is necessarily smaller because of the lack of space. The corresponding cooperative dynamics are in such case faster, that is, occur at higher characteristic frequency, due to a lower degree of cooperativity induced by the small number of molecules present in each pore of the molecular sieves.

The fact that  $T_g$  is lower in the 1 nm pores than in the 0.5 nm pores could be due to that, in the latter case, almost every molecule forms bonds with the internal surface of the MS,

which slows down the dynamics of the prilocaine and water molecules, producing a relatively higher  $T_g$ .

## 4.2 Anti-plasticizing effect of water

Addition of water to PLC produces a systematic and consistent antiplasticizing effect reflected in an increase of  $T_g$ . This is observed not only in the bulk substances but also in the confined systems of 0.5 nm and 1 nm pore size. Whereas the increase of  $T_g$  upon hydration is almost 4 K for bulk PLC, the increase when PLC is confined is 3 K in 0.5 nm pores and 4 K in 1 nm pores.

The result under confinement shed light onto the origin of the antiplasticizing effect.<sup>16</sup> In the molecular sieves where only a few molecules fit the pores, the addition of water to prilocaine produces the formation of nanometric H-bonded clusters rather than more extended networks. It is these hydrated nanoclusters that display collectively a slower dynamics compared with clusters of pure prilocaine. This result is surprising in view of the general plasticizing effect of water, and suggests that extremely tightly bound water–PLC aggregates are formed (e.g., water bridged PLC dimers or trimers). In addition, larger molecular clusters are unlikely to form because of the average size of the cavities. These clusters or aggregates relax as individual units with a larger effective mass and thus a slower reorientational dynamics.

The FTIR results are compatible with this explanation: the H-bond interaction between water and PLC takes place through the carbonyl oxygen,<sup>16</sup> and the absence of a spectral shift of the C=O band of hydrated prilocaine under confinement indicates that such interaction is not affected by confinement, and therefore involves only a low number of molecules inside small-size clusters, rather than an extended H-bond network.

## 5 Conclusions

A rare antiplasticizing effect of water on the prilocaine anesthetic is systematically observed in the bulk as well as when confining the drug inside the nanometric pores of molecular sieves of 0.5 and 1 nm pore size. These results are remarkable considering that only few drug molecules are present in individual pores. The resulting nanosize clusters are responsible for the collective relaxation observed as the  $\alpha$  relaxation in the BDS measurements and thus for the glass transition. This implies that only small clusters are needed in order to observe the antiplasticizing effect.

At the same time, a significant decrease in  $T_g$  upon confinement is observed, which is caused by the reduction of the size of the cooperatively rearranging clusters with respect to the bulk material.

The results presented here may be relevant for drug delivery applications, since they shed light into the effects of nanoconfinement and hydration on a commercial drug, PLC. From a fundamental point of view, our study provides an important insight into the mechanisms that produce the unusual antiplasticizing effect of water on PLC.

## Conflicts of interest

The authors declare no conflict of interest.

## Acknowledgements

The authors thank Isabel Asenjo Sanz for her help when extracting PLC from PLC hydrochloride. This work has been partially supported by the Spanish Ministry of Economy and Competitiveness MINECO through project FIS2017-82625-P and through the project MAT2015-69547-R, and by the Generalitat de Catalunya under project 2017SGR-42. We also thanks Elkartek program (nG17, KK-2017/00012) and the Bask Government under project IT-1175-19.

## Notes and references

- 1 S. Yoshioka and V. J. Stella, *Stability of drugs and dosage forms*, Kluwer Academic Publishers, 2002.
- 2 S. Ewing, A. Hussain, G. Collins, C. Roberts and E. Shalaev, *Low-Temperature Mobility of Water in Sugar Glasses: Insights from Thermally Stimulated Current Study*, Springer, New York, NY, 2016, pp. 75–87.
- 3 H. Levine and L. Slade, *Water Sci. Rev.*, 1988, **3**, 79.
- 4 L. Slade, H. Levine and D. Reid, *Crit. Rev. Food Sci. Nutr.*, 1991, **30**, 79.
- 5 M. Abiad, M. Carvajal and O. Campanella, *Food Eng. Rev.*, 2009, **1**, 105.
- 6 Y. Roos and M. Karel, *J. Food Sci.*, 1991, **56**, 38.
- 7 R. Surana, L. Randall, A. Pyne, N. Vemuri and R. Suryanarayanan, *Pharm. Res.*, 2003, **20**, 1674.
- 8 M. Peleg, *Biotechnol. Prog.*, 1994, **20**, 385.
- 9 C. Angell, *Science*, 1995, **267**, 1924.
- 10 B. Hancock and G. Zografi, *Pharm. Res.*, 1994, **11**, 471.
- 11 C. Angell, *Science*, 2008, **582**, 582.
- 12 M. Gordon and J. Taylor, *J. Appl. Chem.*, 1952, **2**, 493.
- 13 G. Schaumann and E. LeBoeuf, *J. Environ. Sci. Technol.*, 2005, **39**, 800.
- 14 J. Perdomo, A. Cova, A. Sandoval, L. García, E. Laredo and A. Müller, *Carbohydr. Polym.*, 2009, **76**, 305.
- 15 X. Li, Z. Chen, Z. Li, Y. Gao, W. Tu, X. Li, Y. Zhang, Y. Liu and L. Wang, *J. Chem. Phys.*, 2014, **141**, 104506.
- 16 G. Ruiz, M. Romanini, A. Hauptmann, T. Loerting, E. Shalaev, J. L. Tamarit, L. C. Pardo and R. Macovez, *Sci. Rep.*, 2017, **7**, 7470.
- 17 A. Brodin, A. Nyqvist-Mayer, T. Wadsten, B. Forslund and F. Broberg, *J. Pharm. Sci.*, 1984, **73**, 73.
- 18 A. Nyqvist-Mayer, A. Brodin and S. Franck, *J. Pharm. Sci.*, 1985, **74**, 1192.
- 19 A. Nyqvist-Mayer, A. Brodin and S. Franck, *J. Pharm. Sci.*, 1986, **75**, 365.
- 20 I. Rietveld, M. Perrin, S. Toscani, M. Barrio, B. Nicolai, J. Tamarit and R. Ceolin, *Mol. Pharmaceutics*, 2013, **10**, 1332.
- 21 D. Larsen, H. Parshad, K. Fredholt and C. Larsen, *Int. J. Pharm.*, 2002, **232**, 107.
- 22 A. Silva-Santisteban, N. Steinke, A. Johnston, G. Ruiz, L. Pardo and S. McLain, *Phys. Chem. Chem. Phys.*, 2017, **19**, 12665.
- 23 H. Jansson and J. Swenson, *Eur. Phys. J. E: Soft Matter Biol. Phys.*, 2003, **13**, s01.

- 24 R. Macovez, E. Mitsari, M. Zachariah, M. Romanini, P. Zygouri, D. Gournis and J. Tamarit, *J. Phys. Chem. C*, 2014, **118**, 4941.
- 25 H. Haspel, V. Bugris and A. Kukovecz, *J. Phys. Chem. C*, 2013, **117**, 16686.
- 26 L. Frunza, H. Kosslick, I. Pitsch, S. Frunza and A. Schöhal, *J. Phys. Chem. B*, 2005, **109**, 9154.
- 27 E. Mitsari, M. Romanini, M. Barrio, J. Tamarit and R. Macovez, *J. Phys. Chem. C*, 2017, **109**, 4873.
- 28 P. Macedo, C. Moynihan and R. Bose, *Phys. Chem. Glasses*, 1972, **13**, 171.
- 29 F. Kremer and A. Schönhal, *Broadband Dielectric Spectroscopy*, Springer, 2002.
- 30 Z. Wojnarowska, M. Rams-Baron, J. Knapik, K. Ngai, D. Kruk and M. Paluch, *J. Phys. Chem. B*, 2015, **39**, 12699.
- 31 R. Böhmer, K. Ngai, C. Angell and D. Plazek, *J. Chem. Phys.*, 1993, **99**, 4201.